Article

Oxygenase Activity in the Self-Hydroxylation of (*S*)-2-Hydroxypropylphosphonic Acid Epoxidase Involved in Fosfomycin Biosynthesis

Pinghua Liu, Mark P. Mehn, Feng Yan, Zongbao Zhao, Lawrence Que,, and Hung-wen Liu

J. Am. Chem. Soc., **2004**, 126 (33), 10306-10312• DOI: 10.1021/ja0475050 • Publication Date (Web): 29 July 2004

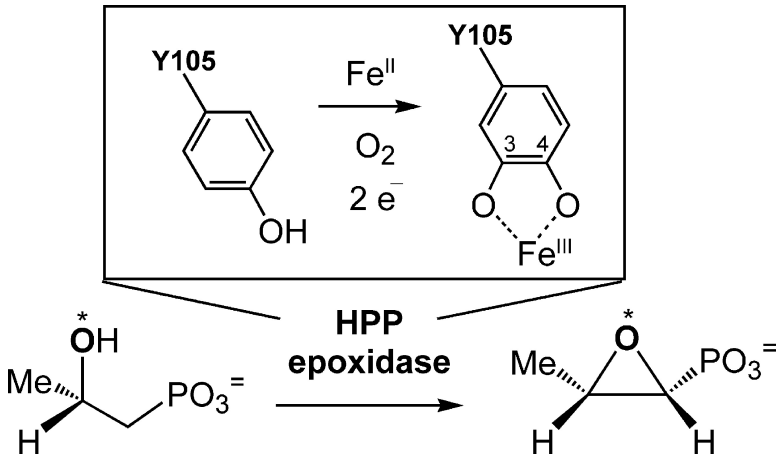

More About This Article

Additional resources and features associated with this article are available within the HTML version:

- Supporting Information
- Links to the 1 articles that cite this article, as of the time of this article download
- Access to high resolution figures
- Links to articles and content related to this article
- Copyright permission to reproduce figures and/or text from this article

View the Full Text HTML

J|A|C|S
ARTICLES
Published on Web 07/29/2004

Oxygenase Activity in the Self-Hydroxylation of (*S*)-2-Hydroxypropylphosphonic Acid Epoxidase Involved in Fosfomycin Biosynthesis

Pinghua Liu,[†] Mark P. Mehn,[‡] Feng Yan,[†] Zongbao Zhao,[†] Lawrence Que, Jr.,*[,‡] and Hung-wen Liu*[,†]

Contribution from the Division of Medicinal Chemistry, College of Pharmacy, and Department of Chemistry and Biochemistry, University of Texas, Austin, Texas 78712, and Department of Chemistry and Center for Metals in Biocatalysis, University of Minnesota, Minneapolis, Minnesota 55455

Received April 29, 2004; E-mail: h.w.liu@mail.utexas.edu

Abstract: The last step of the biosynthesis of fosfomycin is the conversion of (*S*)-2-hydroxypropylphosphonic acid (HPP) to fosfomycin by HPP epoxidase (HppE), which is a mononuclear non-heme iron-dependent enzyme. The apo-HppE from *Streptomyces wedmorensis* is colorless, but turns green with broad absorption bands at 430 and 680 nm after reconstitution with ferrous ion under aerobic conditions. Resonance Raman studies showed that this green chromophore arises from a bidentate iron(III)−catecholate (DOPA) complex, and the most likely site of modification is at Tyr105 on the basis of site-specific mutagenesis results. It was also found that reconstitution in the presence of ascorbate leads to the formation of additional DOPA that shows ^{18}O-incorporation from $^{18}O_2$. Thus, HppE can act as an oxygenase via a putative high valent iron-oxo or an iron-hydroperoxo intermediate, just like other members of the family of non-heme iron enzymes. The oxygen activation mechanism for catalytic turnover is proposed to parallel that for self-hydroxylation.

Non-heme iron enzymes are known to catalyze a range of oxidative reactions more diverse than those associated with heme enzymes.[1,2] Their important roles in many biological processes have stimulated investigations into these non-heme iron enzymes in recent years, resulting in an enhanced understanding of their active site structures, catalytic properties, and mechanisms of action. A large subset of enzymes of this class contains a mononuclear iron(II) center that is coordinated to a recurring 2-His-1-carboxylate facial triad motif.[2,3] These include the extradiol cleaving catechol dioxygenases, α-keto acid-dependent oxidases and oxygenases, pterin-dependent hydroxylases, Rieske-type dioxygenases, the ethylene forming enzyme, and isopenicillin N synthase. Although these enzymes catalyze a wide variety of reactions, their proposed mechanisms all involve a high valent iron-oxo species as oxidant in the course of the overall four-electron reduction of dioxygen to water.[2] An organic cosubstrate, such as ascorbate, tetrahydropterin, or α-ketoglutarate (α-KG), is often required to provide the additional electrons to complete the four-electron redox chemistry.[4−7]

Scheme 1

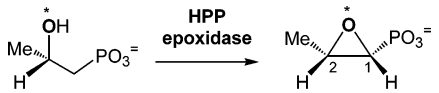

2 **1**

Alternatively, an iron−sulfur cluster, such as that built into Rieske-type dioxygenases,[8] can also be used to mediate electron transfer from NADH. This protein superfamily is expanding rapidly as new enzymes are being discovered.

A recent new candidate for this class is the enzyme (*S*)-2-hydroxypropylphosphonic acid epoxidase (HppE) from *Streptomyces wedmorensis*, which catalyzes the final step of the biosynthesis of fosfomycin (**1**, (1*R*,2*S*)-1,2-epoxypropylphosphonic acid) using (*S*)-2-hydroxypropylphosphonic acid (HPP, **2**) as the substrate (Scheme 1).[9−11] Fosfomycin is a clinically useful antibiotic[12,13] that inhibits the first committed step of bacterial cell wall biosynthesis catalyzed by UDP-*N*-acetylglucosamine enolpyruvyltransferase (MurA in *Escherichia coli*).[14−17]

[†] Division of Medicinal Chemistry, College of Pharmacy, and Department of Chemistry and Biochemistry, University of Texas.
[‡] Department of Chemistry and Center for Metals in Biocatalysis, University of Minnesota.

(1) Solomon, E. I.; Brunold, T. C.; Davis, M. I.; Kemsley, J. N.; Lee, S.-K.; Lehnert, N.; Neese, F.; Skulan, A. J.; Yang, Y.-S.; Zhou, J. *Chem. Rev.* **2000**, *100*, 235−349.
(2) Costas, M.; Mehn, M. P.; Jensen, M. P.; Que, L., Jr. *Chem. Rev.* **2004**, *104*, 939−986.
(3) Hegg. E. L.; Que, L., Jr. *Eur. J. Biochem.* **1997**, *250*, 625−629.
(4) Rocklin, A. M.; Tierney, D. L.; Kofman, V.; Brunhuber, N. M.; Hoffman, B. M.; Christoffersen, R. E.; Reich, N. O.; Lipscomb, J. D.; Que, L., Jr. *Proc. Natl. Acad. Sci. U.S.A.* **1999**, *96*, 7905−7909.
(5) Fitzpatrick, P. F. *Annu. Rev. Biochem.* **1999**, *68*, 355−381.
(6) Kappock, T. J.; Caradonna, J. P. *Chem. Rev.* **1996**, *96*, 2659−2756.
(7) Prescott, A. G.; Lloyd, M. D. *Nat. Prod. Rep.* **2000**, *17*, 367−383.
(8) Gibson, D. T.; Parales, R. E. *Curr. Opin. Biotechnol.* **2000**, *11*, 236−243.
(9) Hidaka, T.; Goda, M.; Kuzuyama, T.; Takei, N.; Hidaka, M.; Seto, H. *Mol. Gen. Genet.* **1995**, *249*, 274−280.
(10) Liu, P.; Murakami, K.; Seki, T.; He, X.; Yeung, S.-M.; Kuzuyama, T.; Seto, H.; Liu, H.-w. *J. Am. Chem. Soc.* **2001**, *123*, 4619−4620.
(11) Liu, P.; Liu, A.; Yan, F.; Wolfe, M. D.; Lipscomb, J. D.; Liu, H.-w. *Biochemistry* **2003**, *42*, 11 577−11 586.
(12) Itoh, N.; Kusaka, M.; Hirota, T.; Nomura, A. *Appl. Microbiol. Biotechnol.* **1995**, *43*, 394−401.
(13) Patel, S. S.; Balfour, J. A.; Bryson, H. M. *Drugs* **1997**, *53*, 637−656.

10.1021/ja0475050 CCC: $27.50

The HppE catalyzed transformation (**2** → **1**) is unusual because the epoxide ring in **1** is formed via a transformation that is essentially a dehydrogenation reaction with retention of the secondary hydroxyl oxygen of **2** in the product.[11,18,19] Unlike most mononuclear non-heme iron enzymes, which utilize an organic cosubstrate or Rieske center to aid in oxygen activation, HppE has no built-in iron−sulfur cluster and is ascorbate-, pterin-, and α-KG-independent. Instead, its catalytic turnover consumes a stoichiometric amount of NADH with molecular oxygen as the oxidant.[10,11] A reductase, whose identity remains elusive, is also required to mediate electron transfer from NADH to the epoxidase.[10] Clearly, the reaction catalyzed by HppE is beyond the scope currently encompassed by common biological epoxidation and C−O bond formation reactions, so HppE is in a class of its own within the mononuclear non-heme iron enzyme superfamily.

In our earlier studies,[11] we have found that the heterologously expressed HppE is an apo-protein. This tetrameric enzyme can be reconstituted with $Fe^{II}(NH_4)_2(SO_4)_2$ to a 1:1 ratio of iron per enzyme monomer. The anaerobically reconstituted Fe(II)-enzyme is colorless, but it develops a green color upon air exposure in the absence of substrate.[11] Here, quinone staining and resonance Raman spectroscopic techniques are used to determine the identity of this green chromophore and to study its biogenesis. This report describes evidence uncovering an Fe(III)−catecholate complex as the chromophoric core, and Tyr105 as the most likely site of post-translational modification to dihydroxyphenylalanine (DOPA). Also included are the possible mechanisms of DOPA formation and the implications on the catalytic mechanism of HppE.

Materials and Methods

General. HppE was purified from *Escherichia coli* BL21(DE3)/pPL1001 according to the published procedure.[11] The enzyme activity was determined as previously described.[10,11] Enzyme E_3 (AscD) used in the assay was purified from the *E. coli* JM105/pOPI cultures based on a procedure published earlier.[20] Protein concentrations were determined by the procedure of Bradford[21] using bovine serum albumin as the standard. DNA sequencing was carried out by the Core Facility of the Institute for Cellular and Molecular Biology, University of Texas at Austin. Culture medium ingredients were purchased from Difco (Detroit, MI). All reagents and solvents were purchased from commercial sources and were used without further purification unless otherwise noted. Biochemicals including fosfomycin disodium salt standard (**1**) were purchased from Sigma (St. Louis, MO). The substrate of HppE, (*S*)-2-hydroxypropylphosphonic acid (**2**), was chemically synthesized according to a procedure reported by Hammerschmidt.[22] Labeled water (95% ^{18}O) and labeled oxygen (99% ^{18}O) were obtained from ICON, Inc (Summit, NJ).

Preparation of HppE Mutants. Site-directed mutagenesis of the HppE gene (*fom4*) was carried out using QuickChange Site-directed Mutagenesis Kit from Strategene (La Jolla, CA). The oligonucleotide primers used for mutagenesis were custom-made by Invitrogen (Carlsbad, CA). These include pKZF1/pKZF2 for Y102F, pKZF3/pKZF4 for Y103F, pKZF5/pKZF6 for Y105F mutant, and pFYF7/pFYF8 for Y103/105F double mutant (pKZF1: 5′-GGACAACGT-CGACTTCTACGTC-TACAACTGTCTC-3′; pKZF2: 5′-CGAGACAGTTGTAGACGTA-GAA-GTCGACGTTGTC-3′; pKZF3: 5′-GGACAACGTCGACTACTT-CGTCTACAACTGTCTC-3′; pKZF4: 5′-CGAGACAGTTGTAGAC-GAAGTAGTCGACGTTGTC-3′; pKZF5: 5′-GTCGAC-TACTACGTCT-TCAACTGTCTCGTCCGC-3′; pKZF6: 5′-CGGACGAGACAGT-TGAAGAC-GTAGTAGTCGACG-3′; pFYF7: 5′-CAACGTCGACTA-CTTCGTCTTCAACTGTCTCGTCC-3′; pFYF8: 5′-GGACGAGA-CAGTTGAAGACGAAGTAGTCGACGTTG-3′). Mutant plasmids were constructed by PCR amplification of the HppE gene from pPL1001 using the above primers under the following conditions: (1) 14 cycles at 95 °C for 30 s, 55 °C for 1 min, and 68 °C for 10 min; (2) 1 cycle at 72 °C for 10 min. The PCR template in each sample was digested with *Dpn*I at 37 °C for 1 h and the recombinant plasmid was then used to transform *E. coli* XL1-blue supercompetent cells. After their sequences were confirmed by DNA sequencing, these mutant plasmids were used to transform *E. coli* BL21(DE3) competent cells for expression. The mutant proteins were purified according to the same procedure used for the wild-type HppE. After reconstitution with $Fe^{II}(NH_4)_2(SO_4)_2$, the excess metals were removed by a G-10 column. The resultant proteins were stored at −80 °C.

NBT Staining of HppE and Its Mutants. The wild-type HppE and its mutants were subjected to 15% SDS-PAGE and transblotted onto a nitro-cellulose membrane at 100 V for 1 h using a transfer buffer (25 mM Tris base, 192 mM glycine, 20% methanol). Detection of the presence of quinoid structure was performed according to a procedure of Paz et al.[23] by immersing the membrane in a solution of 0.24 mM nitroblue tetrazolium and 2 M potassium glycinate, pH 10, for 45 min. After the membrane was rinsed with H_2O, the stained bands were recorded.

Preparation of Enzyme Samples. The apo-enzyme used for resonance Raman studies was prepared by adjusting the apo-HppE solution in 50 mM Tris·HCl buffer (pH 7.5) to a final concentration of 15−20 mg/mL. The apo-protein sample was made anaerobic by repeated cycles of vacuum and purging with argon, and then transferred to the spinning cell (∼150 μL) used for Raman study. The Fe^{II}−HppE sample was prepared by reconstituting the apo-enzyme with 1 equiv. (relative to HppE subunit) of $Fe^{II}(NH_4)_2(SO_4)_2$ in H_2O. This colorless protein solution was exposed to dioxygen for at least 30 min, during which time a green color developed. The protein sample was then concentrated prior to filling the spinning cell. The $H_2{}^{18}O$ samples were prepared by the same procedure except the apo-HppE was lyophilized and reconstituted with $Fe^{II}(NH_4)_2(SO_4)_2$ in $H_2{}^{18}O$ (95% ^{18}O).

Spectroscopic Studies. Electronic absorption spectra were obtained on a HP 8453 diode array spectrometer. Resonance Raman spectra were collected on an Acton AM-506 spectrometer (1200 groove grating) using a Kaiser Optical holographic super-notch filter with a Princeton Instruments liquid N_2 cooled (LN-1100PB) CCD detector with a 4 cm^{-1} spectral resolution. The laser excitation lines were obtained with a Spectra Physics 2030−15 argon ion laser and a 375B CW dye (Rhodamine 6G), or a Spectra Physics BeamLok 2060-KR-V krypton ion laser. The Raman frequencies were referenced to indene, and the entire spectral range of 400−1700 nm was obtained by collecting spectra at 2−3 different frequency windows and splicing the spectra together. All data were referenced to the nonresonance enhanced 1005 cm^{-1} band assigned to a phenylalanine ring mode prior to splicing to avoid artifacts.[24] Raman spectra of HppE were obtained at room temperature by 90° scattering from a spinning cell. Curve fits (Gaussian functions) and baseline corrections (polynomial fits) were carried out using Grams/32 Spectral Notebase Version 4.04 (Galactic). Excitation

(14) Kahan, F. M.; Kahan, J. S.; Cassidy, P. J.; Kropp, H. *Ann. N. Y. Acad. Sci.* **1974**, *235*, 364−386.
(15) Wanke, C.; Amrhein, N. *Eur. J. Biochem.* **1993**, *218*, 861−870.
(16) Marquardt, J. L.; Brown, E. D.; Lane, W. S.; Haley, T. M.; Ichikawa, Y.; Wong, C.-H.; Walsh, C. T. *Biochemistry* **1994**, *33*, 10 646−10 651.
(17) Kim, D. H.; Lees, W. J.; Kempsell, K. E.; Lane, W. S.; Duncan, K.; Walsh, C. T. *Biochemistry* **1996**, *35*, 4923−4928.
(18) Hammerschmidt, F.; Bovermann, G.; Bayer, K. *Liebigs. Ann. Chem.* **1990**, *11*, 1055−1061.
(19) Hammerschmidt, F. *J. Chem. Soc., Perkin Trans. 1* **1991**, *8*, 1993−1996.
(20) Ploux, O.; Lei, Y.; Vatanen, K.; Liu, H.-w. *Biochemistry* **1995**, *34*, 4159−4168.
(21) Bradford, M. M. *Anal. Biochem.* **1976**, *72*, 248−254.
(22) Hammerschmidt, F. *Monatsh. Chem.* **1991**, *122*, 389−398.
(23) Paz, M. A.; Flückiger, R.; Boak, A.; Kagan, H. M.; Gallop, P. M. *J. Biol. Chem.* **1991**, *266*, 689−692.
(24) Lord, R. C.; Yu, N.-T. *J. Miol. Biol.* **1970**, *50*, 509−524.

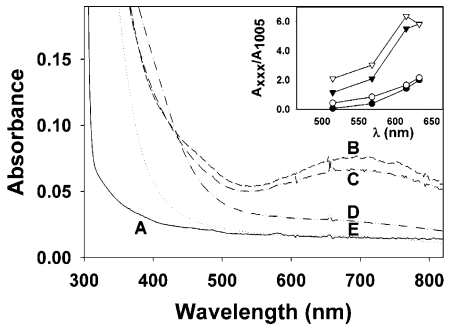

Figure 1. Electronic absorption spectra of apo and Fe-reconstituted HppE (0.15 mM) in 20 mM Tris·HCl buffer, pH 7.5. (A) apo-HppE; (B) HppE + Fe^{II} + O_2; (C) HppE-Y102F + Fe^{II} + O_2; (D) HppE-Y103F + Fe^{II} + O_2; (E) HppE-Y105F + Fe^{II} + O_2. Inset: resonance Raman excitation profiles for the Fe-reconstituted WT HppE. The spectra were obtained on a 1 mM sample in a spinning cell at room temperature (90° scattering geometry). Only profiles for the bands at 592 (●), 635 (○), 1319 (▼), and 1475 (♦) cm^{-1} are shown for clarity. The 1005 cm^{-1} phenylalanine vibration was used as the internal standard and the areas of the peaks were determined by curve fitting.

profiles were constructed by comparing peak area to the nonresonance enhanced vibration at 1005 cm^{-1}.

Results

Optical Properties of HppE. Both apo-HppE and anaerobically reconstituted Fe^{II}−HppE are nearly transparent above 300 nm (Figure 1A). However, upon exposure to molecular oxygen, a green chromophore is formed with visible absorption maxima at 680 and 430 nm within an hour (Figure 1B). Similar chromophores have been observed in tyrosine hydroxylase complexed with various catecholamines (λ_{max} at 420 and 700 nm, ϵ_{720} = 1900 $M^{-1}cm^{-1}$/Fe),[25] in ribonucleotide reductase R2 DOPA208 mutant (λ_{max} at 460 and 720 nm, ϵ_{720} = 2500 $M^{-1}cm^{-1}$ per R2 subunit),[26] and in the iron-substituted zinc-dependent recombinant phosphomannose isomerase (PMI) (λ_{max} at 420 and 680 nm; ϵ_{680} = 2100 $M^{-1}cm^{-1}$ /Fe).[27] These features are all characteristic of an iron(III) center with a chelated catecholate and arise from the catecholate-to-iron(III) charge-transfer transitions.[28,29] However, the Fe−HppE chromophore has a significantly lower extinction coefficient (ϵ_{680} = 450 $M^{-1}cm^{-1}$) than those observed for proteins listed above and model complexes (ϵ = 1500−2500 $M^{-1}cm^{-1}$),[30] suggesting only partial formation of the chromophore in HppE. Another example is taurine/α-KG dioxygenase (TauD) which, along with its cofactor α-KG, reacts slowly with oxygen in the absence of its substrate taurine. This reaction results in the hydroxylation of a nearby tyrosine residue to give rise to a green-brown iron-(III)-catecholate chromophore with λ_{max} at 550 nm and a low extinction coefficient (ϵ = 460 $M^{-1}cm^{-1}$).[31]

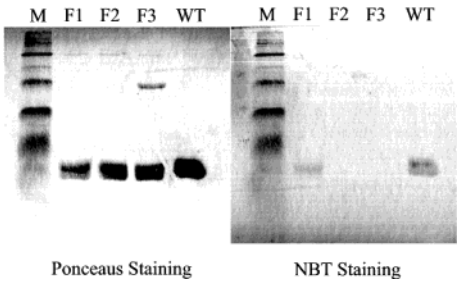

Figure 2. Ponceaus (left) and NBT (right) staining of the wild type HppE and its mutants: lane M, marker bands; lane F1, HppE-Y102F; lane F2, HppE-Y103F; lane F3, HppE-Y105F; lane WT, wild type HppE. The extra band in lane F3 is likely the dimer of HppE-Y105F.

Detection of the Catecholate Residue in HppE by Quinone Staining. Evidence for such a catecholate moiety in HppE was obtained by subjecting the isolated HppE to Paz's quinone-staining reagents including glycine and nitroblue tetrazolium (NBT).[23] It has been shown that under basic conditions, quinone cofactors, such as pyrroloquinoline quinone (PQQ), can oxidize glycine. The reduced quinone can then react with dioxygen to generate superoxide, which in turn oxidizes NBT to formazan to give a blue-purple color. Besides PQQ, other quinonoid compounds, such as 1,2,4-trihydroxybenzene, menadione, and DOPA, are also sensitive to this NBT/glycinate staining method. As shown in Figure 2, HppE is clearly sensitive to the quinone staining treatment. The fact that HppE without reconstitution is strongly stained by NBT/glycinate (see Figure 2, lane WT) not only provides evidence for the presence of a catecholate moiety, but also serves as an initial hint for its formation as an in vivo post-translational event.

Resonance Raman Studies of HppE. To ascertain whether the HppE chromophore consists of a catecholate ligand, the reconstituted Fe^{III}−HppE was subjected to resonance Raman analysis by laser excitation into the green chromophore. The spectrum of the reconstituted protein displays a number of resonance-enhanced features at 533, 588, 635, 1267, 1318, 1425, and 1476 cm^{-1} (Figure 3). This spectrum could be observed with laser wavelengths at 514.5 nm and above, but a high fluorescence background obscured the spectrum when excitation was performed at wavelengths below 514.5 nm. Excitation profiles for selected bands are shown in the inset of Figure 1. By comparison with the thoroughly investigated resonance Raman features of iron(III)−phenolate and iron(III)−catecholate chromophores in both model complexes and enzymatic systems,[28−30] those observed for HppE are characteristic of an iron(III)−catecholate complex and distinct from those of an iron-(III)−phenolate complex (Table 1). The latter displays a different pattern of vibrations from those observed for oxidized HppE, in particular, the presence of only a single ν_{Fe-O} mode in the 560−640 cm^{-1} range, as well as a δ_{C-H} mode at ∼1160 cm^{-1}.[28−30,32] Most of the bands in the region of 1200−1500 cm^{-1} observed for HppE are assignable to aromatic ring deformation modes with predominant ν_{C-C} stretching character and closely match those observed for the ferric-catecholate complexes of phenylalanine hydroxylase,[30] tyrosine hydroxylase,[32] and ribonucleotide reductase R2 DOPA208 mutant[33] (see Table 1). The enhanced vibrational modes between 500 and 700 cm^{-1}, which are associated with metal−ligand vibra-

(25) Andersson, K. K.; Cox, D. D.; Que, L., Jr.; Flatmark, T.; Haavik, J. *J. Biol. Chem.* **1988**, *263*, 18 612−18 626.
(26) Ormö, M.; deMaré, F.; Regnström, K.; Åberg, A.; Sahlin, M.; Ling, J.; Loehr, T. M.; Sanders-Loehr, J.; Sjöberg, B.-M. *J. Biol. Chem.* **1992**, *267*, 8711−8714.
(27) Smith, J. J.; Thomson, A. J.; Proudfoot, A. E. I.; Wells, T. N. C. *Eur. J. Biochem.* **1997**, *244*, 325−333.
(28) Que, L., Jr. In *Biological Applications of Raman Spectroscopy*; Spiro, T. G., Ed.; Wiley: New York, 1988; Vol. 3, pp 491−521.
(29) Pyrz, J. W.; Roe, A. L.; Stern, L. J.; Que, L., Jr. *J. Am. Chem. Soc.* **1985**, *107*, 614−620.
(30) Cox, D. D.; Benkovic, S. J.; Bloom, L. M.; Bradley, F. C.; Nelson, M. J.; Que, L., Jr.; Wallick, D. *J. Am. Chem. Soc.* **1988**, *110*, 2026−2032.
(31) Ryle, M. J.; Liu, A.; Muthukumaran, R. B.; Ho, R. Y. N.; Koehntop, K. D.; McCracken, J.; Que, L., Jr.; Hausinger, R. P. *Biochemistry* **2003**, *42*, 1854−1862.
(32) Michaud-Soret, I.; Andersson, K. K.; Que, L., Jr. *Biochemistry* **1995**, *34*, 5504−5510.

Table 1. Resonance Raman Vibrations of Iron(III)-Catecholates in Proteins and Models

sample	Raman frequencies (cm^{-1})									ref
HPP epoxidase + Fe + $^{16}O_2$	533	588	635		1267	1318	1425	1476		this work
HPP epoxdiase + Fe + $^{18}O_2$	532	587	635		1267	1319	1425	1477		this work
HPP epoxidase + Fe + $^{16}O_2$ + $H_2{}^{18}O$	534	588	636		1266	1317	1425	1476		this work
HPP epoxidase + Fe + Asc + $^{16}O_2$	531	591	636		1264	1315	1425	1478		this work
HPP epoxidase + Fe + Asc + $^{18}O_2$	525	570	633		1261	1315	1424	1478		this work
RNR R2 DOPA-208	512	592	619	1143	1263	1319	1350	1475	1569	33
RNR R2 [3-^{18}O, 4-^{16}O]DOPA-208	499	584	617	1143	1263	1319	1350	1475	1569	33
Phe hydroxylase + catecholate	531		621	1151	1257	1313		1470	1568	30
Tyr hydroxylase DOPA	528	592	631		1275	1320	1425	1475		32
Tyr hydroxylase [3-^{18}O, 4-^{16}O]DOPA	522	580	629		1271	1320	1425	1475		32
Tyr hydroxylase [3-^{18}O, 4-^{18}O]DOPA	509	578	619		1266(br)	1320	1423	1473		32
phosphomannose isomerase DOPA-287		591	631		1266	1330	1428	1482		27
TauD DOPA-73	545		612	1141	1261	1318 1346	1424	1482		31
[Fe^{III}(salen)(catecholate)]$^-$	511		614		1260	1324		1473		29
[Fe^{III}(catecholate)$_3$]$^{3-}$	533		622		1267	1327		1487		34

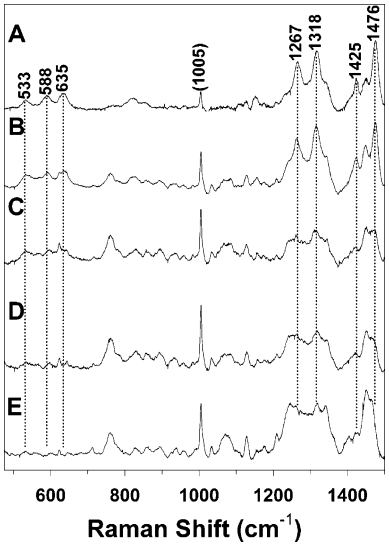

Figure 3. Resonance Raman spectra of (A) wild-type HppE + Fe^{II} + O_2, (B) HppE-Y102F + Fe^{II} + O_2, (C) HppE-Y103F + Fe^{II} + O_2, (D) HppE-Y105F + Fe^{II} + O_2, and (E) apo HppE, obtained using 632.8 nm laser excitation with 90° scattering geometry from a spinning cell at room temperature. The spectra are not shown at the same vertical scale (note changes in the intensity of the 1005 cm^{-1} band associated with the Phe residues in the enzyme that serves as an internal calibrant of protein concentration).

tions (ν_{Fe-O}), are the most significant signals for the identification of the iron-catecholate chromophore.[34] The peaks at 635 and 588 cm^{-1} can be assigned to the Fe−O stretches at C-4 and C-3 of the DOPA catecholate ring, respectively, and the feature at 533 cm^{-1} arises from the chelate mode of a bidentate iron-catecholate species.[30,32,33] Thus, the resonance Raman spectrum of HppE is fully consistent with the presence of an iron-catecholate chromophore.

Determination of the Site of Modification by Site-Directed Mutagenesis. The catecholate moiety in HppE presumably arises from the hydroxylation of a tyrosine residue. Interestingly, sequence alignment of HppE from *Streptomyces wedmorensis* and *Pseudomonas syringae* reveals only three conserved tyrosine residues, Y102, Y103, and Y105 (Figure 4). Site-directed mutagenesis of each tyrosine to phenylalanine has thus been carried out to determine which of the three conserved tyrosine residues is involved in the formation of the chromophore. The reconstituted Y102F mutant enzyme is green in color and has a visible as well as a resonance Raman spectrum comparable to those of the wild-type enzyme (Figures 1C and 3B), so Y102 can be ruled out as the site of modification. On the other hand, the reconstituted Y103F and Y105F mutant enzymes show little evidence for the green chromophore in their visible spectra (Figures 1D, 1E), and their Raman spectra are comparable to that observed for apo-HppE (Figures 3C, 3D, and 3E). Thus, either Y103 or Y105 can be the precursor of DOPA in HppE (see Schemes 2 and 3). This conclusion is corroborated by parallel quinone staining experiments. As shown in Figure 2, both the wild type (lane WT) and Y102F (lane F1) HppE are stained, but not Y103F (lane F2) and Y105F (lane F3) mutant enzymes. Interestingly, whereas the Y102F and Y103F enzymes maintain about 60% of the activity of the wild type enzyme, the Y105F enzyme is essentially inactive. Clearly, Tyr105 is a key residue, which plays a role in the activation of dioxygen required for the enzymatic activity of HppE.

Post-translational DOPA Formation in Vivo and/or in Vitro. To gain more information about this post-translational modification event, more Raman experiments were performed using HppE samples reconstituted with isotopic tracers, for instance under $^{18}O_2$ atmosphere in $H_2{}^{16}O$, and under $^{16}O_2$ atmosphere in $H_2{}^{18}O$. Neither notable broadening nor significant isotopic shifting of the peaks was observed in any of the tested samples (see Table 1 and Figure 5A−C). The absence of isotope incorporation in these samples confirms that formation of DOPA in HppE is not an artifact of in vitro reconstitution but an in vivo post-translational event.

However, when reconstitution was carried out under $^{18}O_2$ atmosphere in the presence of ascorbate (10 equiv), the green chromophore increased in intensity and isotope shifts for several Raman peaks were observed (Figure 5D,E). The change at 591 cm^{-1} is most apparent, with the appearance of the new peak at 570 cm^{-1} (see Table 1). This peak can be attributed to the ^{18}O downshift of the 591 cm^{-1} peak, which corresponds to the Fe(III)-OAr stretch at C-3 of the DOPA ring, owing to ^{18}O incorporation. The feature at 531 cm^{-1} assigned to the iron-catecholate chelate mode also downshifts by 6 cm^{-1} and broadens significantly to a width twice as large as that observed in the $^{16}O_2$ sample. Downfield shifts of 3 cm^{-1} are also observed for the Fe−O_4 mode at 636 cm^{-1} and the ring deformation mode at 1264 cm^{-1}. These isotopic shifts are reminiscent of those observed in the spectrum of tyrosine hydroxylase when com-

(33) Ling, J.; Sahlin, M.; Sjöberg, B.-M.; Loehr, T. M.; Sanders-Loehr, J. *J. Biol. Chem.* **1994**, *269*, 5595−5601.
(34) Salama, S.; Stong, J. D.; Neilands, J. B.; Spiro, T. G. *Biochemistry* **1978**, *17*, 3781−3785.

```
S. wendomorensis    MSNTKTASTG FAELLKDRRE QVKMDHAALA SLLGETPETV AAWENGEGGE   50
P. syringae         M-DVRTLAVG KAH-LEALLA TRKM---TLE HLQDVRHDAT QVYFDGLEHL   45
Consensus           M....T...G .A..L..... ..KM....L. .L........ .....G....   50

S. wendomorensis    LTLTQLGRIA HVLGTSIGAL TPPAGNDLDD GVIIQMPDER PILKGVRDNV  100
P. syringae         QNVAQY--LA IPLSEFFVGQ TQ---SDLDD GVKIARRNGG FKREEIRGGV   90
Consensus           ....Q....A ..L....... T.....DLDD GV.I...... ......R..V  100

S. wendomorensis    DYYVYNCLVR TKRAPSLVPL VVDVLTDNPD DAKFNSGHAG NEFLFVLEGE  150
P. syringae         HYYTYEHLVT TNQDPGLMAL RLDLHSDDEQ PLRLNGGHGS REIVYVTRGA  140
Consensus           .YY.Y..LV. T...P.L..L ..D...D... ....N.GH.. .E...V..G.  150

S. wendomorensis    IHMKW-GDKE NPKEALLPTG ASMFVEEHVP HAFTAAKGTG SAKLIAVNF-  198
P. syringae         VRVRWVGDND ELKEDVLNEG DSIFILPNVP HSFTNHVGGA KSEIIAINYG  190
   Consensus        ....W.GD.. ..KE..L..G .S.F....VP H.FT...G.. ....IA.N..  200
```

Figure 4. Sequence alignment of HppE isolated from *Streptomyces wedmorensis* and *Pseudomonas syringae*. The three conserved tyrosines are boxed and residues likely to constitute the proposed 2-His-1-carboxylate facial triad are underlined.

Scheme 2

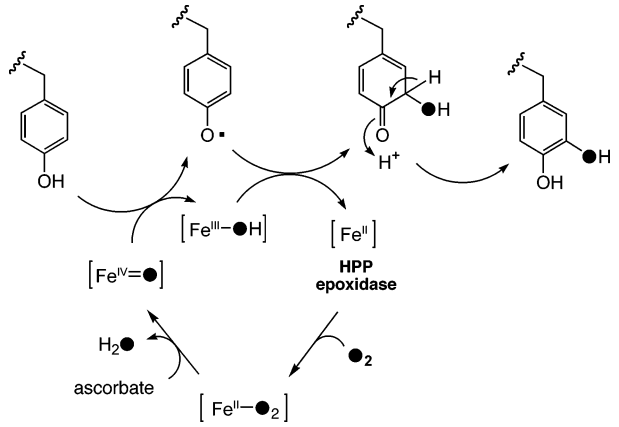

Scheme 3

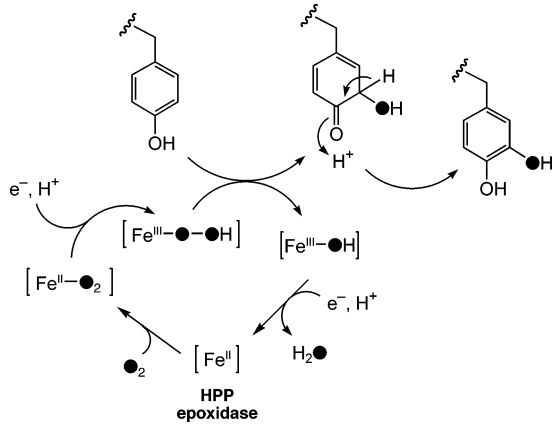

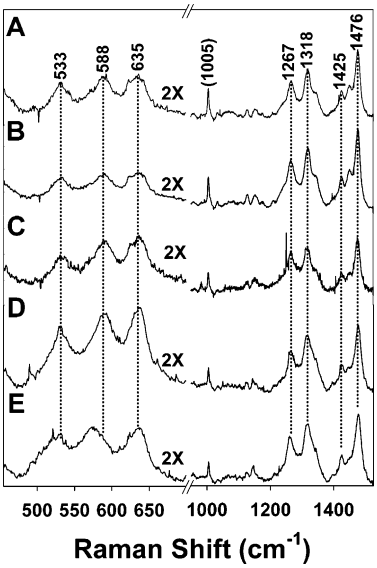

Figure 5. Resonance Raman spectra of reconstituted HppE: (A) HppE + Fe^{II} + $^{16}O_2$, (B) HppE + Fe^{II} + $^{18}O_2$, (C) HppE + Fe^{II} + $^{16}O_2$ + $H_2{}^{18}O$, (D) HppE + Fe^{II} + $^{16}O_2$ and 10 equiv of ascorbate, and (E) HppE + Fe^{II} + $^{18}O_2$ and 10 equivalents of ascorbate. The vertical scale in the lower region has been magnified to two times that of the upper region for clarity. A greater number of accumulations were acquired for the $H_2{}^{18}O$ sample.

plexed with dopamine specifically labeled at the 3-position of the aromatic ring (Table 1).[32]

These results clearly indicate that HppE is capable of catalyzing tyrosine self-hydroxylation when provided with sufficient electrons for oxygen activation. However, due to the tight binding between ascorbate and the iron center to form an aborted complex, HppE reconstituted under such conditions is catalytically inactive.

Reconstitution of Mutant Proteins in the Presence of Ascorbate. Taking advantage of the newly discovered oxygenase activity of HppE, the Y103F, Y105F, and Y103F/Y105F mutant proteins were also subjected to aerobic reconstitution with $Fe^{II}(NH_4)_2(SO_4)_2$ in the presence of ascorbate (10 equiv) to further differentiate between Tyr103 and Try105 as the site of modification. After 1-h incubation, the Y103F mutant protein became green in color and its electronic absorption spectrum clearly revealed the formation of the green chromophore with the maximum wavelength at 680 nm (ϵ_{680} = 360 $M^{-1}cm^{-1}$, Figure 6A). In contrast, much less green chromophore was produced from the Y105F mutant under the same conditions (ϵ_{680} = 200 $M^{-1}cm^{-1}$, Figure 6B). The spectrum of the wild-type HppE at the same concentration is also included (ϵ_{680} = 450 $M^{-1}cm^{-1}$, Figure 6D) for comparison. These observations strongly indicate that Tyr105 is the preferred site of modification. However, the fact that the absorption at longer wavelength remains visible for the reconstituted Y105F mutant suggests that hydroxylation at the nearby Tyr103 can occur when Tyr105 is mutated to a less reactive phenylalanine. This hypothesis is supported by the finding that the Y103F/Y105F double mutant showed no sign of modification under the same reconstitution conditions (Figure 6C).

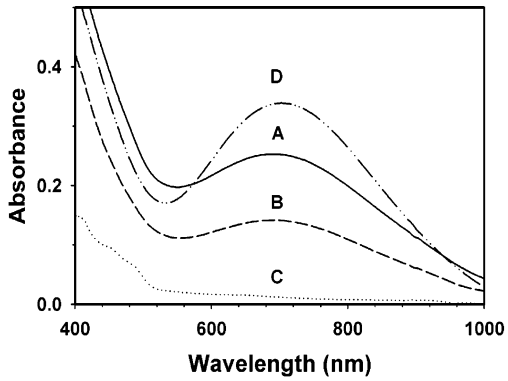

Figure 6. Electronic absorption spectra of WT and mutants HppE (0.6 mM) aerobically reconstituted with Fe^{II} and 10 equiv of ascorbate in 20 mM Tris·HCl buffer, pH 7.5: (A) HppE-Y103F, (B) HppE-Y105F, (C) HppE-Y103F/Y105F, and (D) WT HppE.

Discussion

An increasing number of proteins that are post-translationally modified to contain a DOPA residue have been discovered in recent years. Many DOPA-containing proteins are found in liver flukes or in adhesive plaques of mussels where their DOPA residues play important roles in metal chelation facilitating the iron uptake.[35,36] There are also examples where DOPA formation occurs in enzymes. Such a post-translational modification is well documented for the F208Y mutant of the ribonucleotide reductase (RNR) R2 protein from *E. coli*, where the newly introduced tyrosine residue (Tyr208) near the diiron active site is hydroxylated both in vitro and in vivo to DOPA.[37] The crystal structure of this mutant protein indeed showed a diiron(III) core with a bidentate catecholate ligand (DOPA208) to one of the iron ions that gives rise to its unusual blue color. A tyrosine residue (Tyr287) in the active site of the zinc-dependent recombinant phosphomannose isomerase (PMI) can also be hydroxylated to DOPA in the overexpressed cells to generate a green chromophore when the zinc center is replaced by iron.[27] Similarly, Tyr73 is converted to DOPA in the α-KG-dependent non-heme iron enzyme TauD to generate a green chromophore when the enzyme reacts with O_2 in the presence of α-KG cosubstrate, but in the absence of its substrate taurine.[31] By a combination of site-directed mutagenesis and resonance Raman spectral analysis in this study, we have established HppE as a new member of this select group of proteins with hydroxylated tyrosine residues. The site of modification in HppE is most likely at Tyr105.

Several of the DOPA forming enzymes mentioned above as well as tyrosine hydroxylase belong to a family of mononuclear non-heme iron enzymes with the recurring 2-His-1-carboxylate facial triad in their active sites.[2,3] Sequence comparisons (Figure 4) suggest that HppE likely utilizes the combination of H138, H180, and E142 as ligands to the iron(II) center, thus making it another plausible addition to this family of oxygen activating enzymes. But the reaction it catalyzes is unusual, entailing an oxidative dehydrogenation of HPP (**2**) to form fosfomycin (**1**) such that the alcohol oxygen of the substrate becomes the epoxide ring oxygen in the product (Scheme 1). The lack of any oxygen incorporation from O_2 into the epoxide product (**1**) is somewhat unexpected, as metalloenzyme-catalyzed epoxidations typically result in the incorporation of an oxygen atom from O_2. However, our observation that HppE can carry out the hydroxylation of a tyrosine residue to DOPA in the presence of ascorbate with incorporation of an oxygen atom from O_2 suggests that it may share a common mechanism for oxygen activation with other mononuclear non-heme iron enzymes.[2]

The mechanism of substrate hydroxylation catalyzed by non-heme iron enzymes typically involves a high valent iron-oxo species produced at the expense of two exogenous electrons in each catalytic cycle. For tyrosine hydroxylase, the two electrons are provided by the tetrahydropterin cofactor, and for α-KG-dependent enzymes such as TauD, the two electrons derive from the α-KG cosubstrate. Although the resultant iron(IV)-oxo species is considered the reactive intermediate responsible for tyrosine oxidation in both cases, the actual mechanisms of oxygen incorporation into DOPA may not be the same. For tyrosine hydroxylase where tyrosine is an external substrate, a cationic cyclohexadiene intermediate, perhaps from an arene oxide, is proposed to be the product of the initial oxygen addition.[5] Evidence supporting this concerted oxygen-transfer mechanism includes the occurrence of a NIH shift in the subsequent rearrangement to yield DOPA, and the exclusive incorporation of an oxygen atom from dioxygen into the DOPA structure.[5] In contrast, for self-hydroxylation of TauD where the substrate (Tyr73) is an internal active site residue, the reaction proceeds via a tyrosyl radical intermediate, whose formation is associated with the reduction of the iron(IV)−oxo to an iron(III)−hydroxo species, with exclusive incorporation of an oxygen atom from water into the DOPA that is formed.[31] An oxygen atom from water was also incorporated into a hydroxylated Trp residue in another α-KG-dependent mononuclear non-heme iron containing dioxygenase, TfdA,[38] and into a DOPA residue of RNR R2 F208Y mutant[33] by presumed involvement of an iron(IV)-oxo species.

The self-hydroxylation of HppE may follow a similar path as the above enzymes. An iron(IV)−oxo intermediate may be formed with the influx of two reducing equivalents from ascorbate in place of tetrahydropterin or α-ketoglutarate into the $Fe-O_2$ adduct (Scheme 2). Tyrosine hydroxylation may then occur as a $2e^-$-oxidation as proposed for tyrosine hydroxylase[5] or in two $1e^-$-steps as demonstrated for TauD self-hydroxylation.[31]

However, tyrosine hydroxylase, TauD, and TfdA utilize either tetrahydropterin or α-KG bound at the active site as the two-electron source, whereas HppE instead uses an external reductant, either ascorbate for the in vitro formation of DOPA or NADH for the catalyzed epoxide formation. This requirement for an external reductant resembles that for another class of non-heme iron enzymes with a 2-His-1-carboxylate motif, the Riseke dioxygenases that catalyze *cis*-dihydroxylation of arenes, where the two electrons from NADH are introduced in $1e^-$-aliquots during the catalytic cycle.[2,8] There is recent strong evidence in the Rieske dioxygenase mechanism for an $Fe^{III}-OOH$ intermediate that derives from the one-electron reduction of an initial iron(II)$-O_2$ adduct.[39,40] This peroxo intermediate is proposed

(35) Waite, J. H.; Housley, T. J.; Tanzer, M. L. *Biochemistry* **1985**, *24*, 5010−5014.
(36) Waite, J. H.; Rice-Ficht, A. C. *Biochemistry* **1989**, *28*, 6104−6110.
(37) Åberg, A.; Ormö, M.; Nordlund, P.; Sjöberg, B.-M. *Biochemistry* **1993**, *32*, 9845−9850.
(38) Liu, A.; Ho, R. Y.; Que, L., Jr.; Ryle, M. J.; Hausinger, R. P. *J. Am. Chem. Soc.* **2001**, *123*, 5126−5127.
(39) Karlsson, A.; Parales, J. V.; Parales, R. E.; Gibson, D. T.; Eklund, H.; Ramaswamy, S. *Science* **2003**, *299*, 1039−1042.

to either attack the substrate directly or may evolve first to an iron(V)−oxo species that then carries out the oxidation. HppE self-hydroxylation may also be envisioned to occur by such a pathway (Scheme 3).

In summary, the combined spectroscopy as well as mutagenesis results have identified an iron−catecholate complex as the chromophore for the green color of HppE. More importantly, strong evidence indicates that DOPA formation in HppE is a self-hydroxylation reaction. It is thus clear that HppE can act as an oxygenase and an activated dioxygen species is responsible for the self-hydroxylation. The discovery of this new activity of HppE has significant mechanistic implications since by extension, the same reactive intermediates may be involved in the catalytic mechanism for fosfomycin formation. Adaptation of Schemes 2 and 3 to HppE-catalyzed HPP epoxidation is straightforward and would require the oxidant (either the Fe^{IV}═O species in Scheme 2 or the Fe^{III}−OOH species in Scheme 3) to carry out the $2e^-$-oxidation of substrate in one-electron steps (Scheme 4), parallel to the alkane hydroxylation mechanisms proposed for cytochrome P450[41] and nonheme iron oxygenases.[2] The first step would involve hydrogen-atom abstraction from the C-1 of HPP to generate a substrate radical, followed by epoxide ring formation and concomitant reduction of the metal center in a step reminiscent of oxygen rebound in cytochrome P450.[41] More studies are in progress to uncover details of the DOPA formation mechanism relevant to that of HppE-catalyzed epoxidation. Insight gained from study of this unique non-heme iron-dependent enzyme will certainly enhance our understanding of this important and growing enzyme family.

(40) Wolfe, M. D.; Lipscomb, J. D. *J. Biol. Chem.* **2003**, *278*, 829−835.
(41) Groves, J. T. *J. Chem. Educ.* **1985**, *62*, 928−931.

Scheme 4

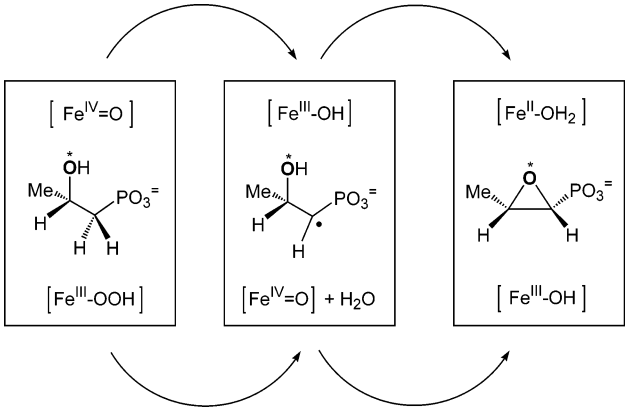

Abbreviations: E_3, CDP-6-deoxy-L-*threo*-D-*glycero*-4-hexulose 3-dehydrase reductase; DOPA, dihydroxyphenylalanine; HPP, (*S*)-2-hydroxypropylphosphonic acid; HppE, (*S*)-2-hydroxy-propylphosphonic acid epoxidase; α-KG, α-ketoglutarate; NADH, *β*-nicotinamide adenine dinucleotide, reduced form; NBT, nitroblue tetrazolium; PAGE, polyacrylamide gel electrophoresis; PCR, polymerase chain reaction; PMI, phosphomannose isomerase; PQQ, pyrroloquinoline quinone; RNR R2, ribonucleotide reductase subunit R2; SDS, sodium dodecyl sulfate; TauD, taurine/α-KG dioxygenase; WT, wild-type.

Acknowledgment. This work was supported in part by grants from the National Institutes of Health (GM40541 to H.-w.L and GM33162 to L.Q.) and a predoctoral traineeship to M.P.M. (GM08700).

JA0475050